Articles

Correlation of Tryptophan Fluorescence Intensity Decay Parameters with ^{1}H NMR-Determined Rotamer Conformations: [Tryptophan^2]Oxytocin†

J. B. Alexander Ross,*,‡ Herman R. Wyssbrod,§,‖ Richard A. Porter,§ Gerald P. Schwartz,‡ Chris A. Michaels,⊥ and William R. Laws*,‡

Department of Biochemistry, Mount Sinai School of Medicine, One Gustave L. Levy Place, New York, New York 10029, and Department of Chemistry, University of Louisville, Louisville, Kentucky 40292

Received August 14, 1991; Revised Manuscript Received November 1, 1991

ABSTRACT: While the fluorescence decay kinetics of tyrosine model compounds [Laws, W. R., Ross, J. B. A., Wyssbrod, H. R., Beechem, J. M., Brand, L., & Sutherland, J. C. (1986) *Biochemistry 25*, 599–607] and the tyrosine residue in oxytocin [Ross, J. B. A., Laws, W. R., Buku, A., Sutherland, J. C., & Wyssbrod, H. R. (1986) *Biochemistry 25*, 607–612] can be explained in terms of heterogeneity derived from the three ground-state χ^1 rotamers, a similar correlation has yet to be directly observed for a tryptophan residue. In addition, the asymmetric indole ring might also lead to heterogeneity from χ^2 rotations. In this paper, the time-resolved and steady-state fluorescence properties of [tryptophan^2]oxytocin at pH 3 are presented and compared with ^{1}H NMR results. According to the unrestricted analyses of individual fluorescence decay curves taken as a function of emission wavelength and a global analysis of these decay curves for common emission wavelength-independent decay constants, only three exponential terms are required. In addition, the preexponential weighting factors (amplitudes) have the same relative relationship (weights) as the ^{1}H NMR-determined χ^1 rotamer populations of the indole side chain. ^{15}N was used in heteronuclear coupling experiments to confirm the rotamer assignments. Inclusion of a linked function restricting the decay amplitudes to the χ^1 rotamer populations in the individual decay curve analyses and in the global analysis confirms this correlation. According to qualitative nuclear Overhauser data, there are two χ^2 populations. Depending upon the degree of correlation between χ^2 and χ^1, there may be from three to six side-chain conformations for the tryptophan residue. The combined fluorescence and NMR results are consistent with a rotamer model in which either (i) the χ^2 rotations are fast compared to the fluorescence intensity decay of the tryptophan residue, (ii) environmental factors affecting fluorescence intensity decay properties are dominated by χ^1 interactions, or (iii) the χ^2 and χ^1 rotations are highly correlated.

Tryptophan is an important intrinsic fluorescence probe that has been widely used to obtain information about the structure and dynamics of proteins and polypeptides in solution. Its fluorescence properties can also be used as experimental observables in quantitation of ligand binding. The usefulness of tryptophan as an intrinsic probe arises in part from the sensitivity of the indole chromophore to the physical and chemical nature of its local environment (Konev, 1967; Longworth, 1971; Creed, 1984). For example, events such as intermolecular association or denaturation are generally accompanied by shifts in the excitation and emission spectra as well as by changes in the quantum yield.

The fluorescence intensity decay kinetics of tryptophan also have the potential of providing structural and chemical information. The interpretation of tryptophan fluorescence decay kinetics, however, is not straightforward. Although some single tryptophan-containing proteins have fluorescence kinetics that obey a monoexponential decay law, the general observation is that most have fluorescence kinetics which are complex (Grinvald & Steinberg, 1976; Beechem & Brand, 1985). This is even observed for the simpler case of the tryptophan zwitterion (Rayner & Szabo, 1978) and its α-amino and α-carboxyl analogues (Szabo & Rayner, 1980; Robbins et al., 1980; Ross et al., 1981a; Chang et al., 1983; Petrich et al., 1983; Chen et al., 1991). One might, therefore, expect that a protein with two or more tryptophan residues would have fluorescence decay kinetics too complicated to be experimentally resolved. However, horse liver alcohol dehydrogenase, a homodimer with two tryptophan residues in each subunit, one residue exposed to solvent, and the other buried at the subunit interface (Brändén et al., 1975), has a fluorescence decay that can be described by a sum of two exponentials (Ross et al., 1981b). In this case, each tryptophan appears to be a single exponential since the short-lived and long-lived decay components can be associated with the buried and exposed tryptophans, respectively (Ross et al., 1981b; Knutson et al., 1982; Eftink & Hagaman, 1986). Consequently, before tryptophan fluorescence can be used to describe protein structure and dynamics, the basis for both simple and complex decay kinetics needs to be understood.

The complex fluorescence decay of the tryptophan zwitterion has been ascribed to several mechanisms, including dual emission from the ^1L_a and the ^1L_b singlet excited states[1] of the

† Supported by a grant from the National Institutes of Health (GM-39750 to J.B.A.R.) and in part by grants from the National Science Foundation for Biological Instrumentation (DMB-8516318 to J.B.A.R.) and Chemical Instrumentation (CHE-8821034 to A. F. Spatola).

* Authors to whom correspondence should be addressed.

‡ Department of Biochemistry, Mount Sinai School of Medicine, New York, NY 10029.

§ Department of Chemistry, University of Louisville, Louisville, KY 40292.

‖ Environmental Sciences Laboratory, Brooklyn College, Brooklyn, NY 11210.

⊥ Present address: Swarthmore College, Swarthmore, PA 19081.

0006-2960/92/0431-1585$03.00/0

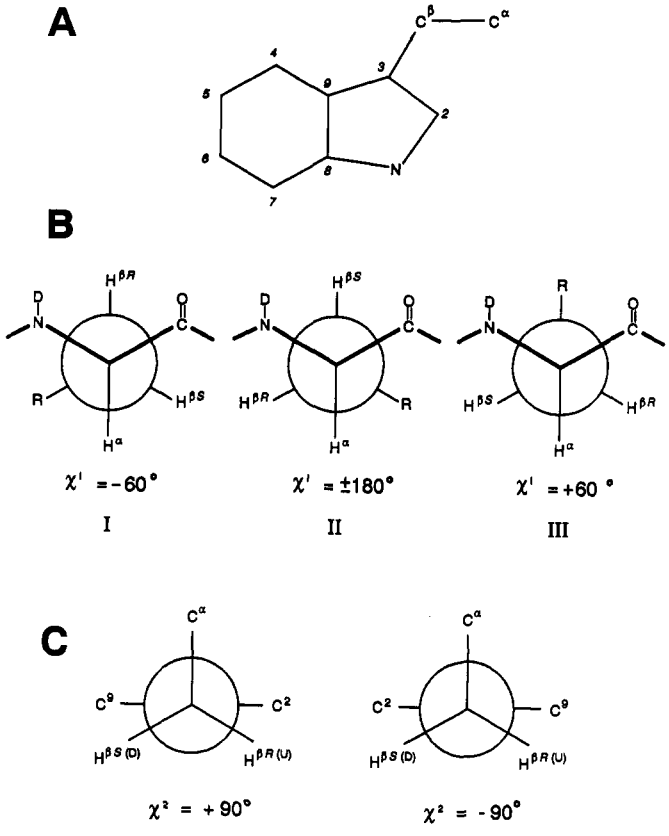

FIGURE 1: (A) Numbering for the carbon backbone of the indole ring of tryptophan. (B) Newman projections about the C^{α}–C^{β} bond where R denotes the possible positions of the indole moiety. The rotamer assignments I, II, and III and the corresponding values of the χ^1 torsion angle are given for the L configuration of tryptophan. The atom D indicates the state of the compound in D_2O, the solvent used for the NMR studies. (C) Newman projections about the C^{β}–C^{γ} bond of tryptophan.

indole ring (Rayner & Szabo, 1978), conformational heterogeneity due to χ^1 rotamers of the tryptophan side chain (Szabo & Rayner, 1980), and intramolecular proton exchange between the protonated α-amino group and the C-4 indole hydrogen (Saito et al., 1984; Shizuka et al., 1988; Chen et al., 1991). (For a description of the χ^1 rotamers and the indole numbering system, see Figure 1.) It has also been suggested that the fluorescence decay kinetics are so complex that they should be represented by a distribution of lifetimes (James & Ware, 1985; Wagner et al., 1987). The results of time-resolved fluorescence studies of tryptophan analogues cooled in supersonic jets, however, indicate monoexponential decays for different conformers (Sipior et al., 1987; Philips et al., 1988). Other evidence suggesting that the complex fluorescence decay of tryptophan may originate from ground-state heterogeneity comes from the elegant studies by Barkley and co-workers (Tilstra et al., 1990; Colucci et al., 1990). They synthesized

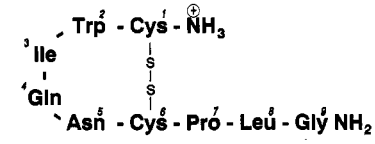

FIGURE 2: Chemical structure of [Trp^2]oxytocin at pH 3.

a tryptophan analogue, 3-carboxy-1,2,3,4-tetrahydro–2–carboline, which has restricted rotation of the alanyl side chain. The fluorescence decay of the zwitterionic form of the analogue is a double exponential, and the preexponential amplitudes correspond closely to the two conformational populations calculated from ^1H NMR[2] coupling constants.

In an earlier study on tyrosine and tyrosine analogues, we examined the possibility that the ground-state χ^1 rotamer populations were correlated with the fluorescence decay kinetics (Laws et al., 1986). We focused on tyrosine because there is no distinction between χ^2 rotamers due to the symmetry of the phenol ring, and there are only the three possible χ^1 side-chain rotamer configurations to provide different environments for the phenol ring. Our results for the tyrosine decay kinetics were consistent with χ^1 ground-state rotamers which interconvert slowly on the fluorescence time scale. We obtained the same correlation comparing the fluorescence decay kinetics and ^1H NMR-determined rotamer populations of the single tyrosine at position 2 (Tyr^2) in the peptide hormone oxytocin (Ross et al., 1986a). Oxytocin, which is involved with lactation and uterine contraction at childbirth, consists of nine amino acids cyclized by a disulfide bond between Cys^1 and Cys^6. Our time-resolved fluorescence results also showed that one of the Tyr^2 χ^1 rotamers interacts with the disulfide bridge and is statically quenched.

To use the fluorescence intensity decay kinetics of tryptophan residues to probe structure requires knowing how different ground-state and excited-state processes affect the intensity decay. At the present time, there is no clear understanding about the relationship between χ^1 and χ^2 rotamer populations and the fluorescence intensity decay of a tryptophan residue in a polypeptide or protein. Due to the asymmetry of the indole ring, the χ^2 rotamers of tryptophan are distinct; a total of six possible χ^1 and χ^2 rotamer configurations (Figure 1) has been confirmed by ^1H NMR (Dezube et al., 1981). Different rotamer configurations should result in different environments for the indole chromophore since each configuration will yield different interactions of the indole ring with the peptide backbone and substituent groups such as disulfides and other side chains, as well as the possibility of different degrees of solvation. If interconversion among these configurations is slow compared to the rate of the fluorescence intensity decay, we would expect a correlation between the fluorescence decay parameters and the ^1H NMR-determined ground-state rotamer populations (Ross et al., 1988).

To test the hypothesis that ground-state rotamers contribute to the complex fluorescence intensity decay of tryptophan residues, we have synthesized an analogue of oxytocin in which Tyr^2 is replaced with tryptophan ([tryptophan^2]oxytocin or [Trp^2]oxytocin; see Figure 2). Oxytocin was selected as a model system to study the fluorescence decay of a tryptophan residue because [Tyr^2]oxytocin has been extensively charac-

[1] The lowest energy absorption band of the indole ring includes two $\pi^* \leftarrow \pi$ transitions to overlapping excited singlet states which, according to Platt's notation, are designated ^1L_a and ^1L_b (Platt, 1949, 1951). Valeur and Weber (1977) resolved these bands by fluorescence polarization spectroscopy of samples in rigid propylene glycol at 215 K. According to studies by Strickland and co-workers (Strickland et al., 1970, 1972), as well as by others (Leonard & Forster, 1974; Sun & Song, 1977; Suzuki et al., 1977; Tatischeff et al., 1978; Lami & Glasser, 1986), the ^1L_a band is affected more strongly by solvent interactions and is generally at lower energies in polar solvents. Rehms and Callis (1987) have also compared the energies of the ^1L_a and ^1L_b excitation transitions of several methyl indoles using two-photon spectroscopy. Their results confirm the relative responses of these two transitions to solvents of varying polarity.

[2] Abbreviations: ^1H NMR, proton nuclear magnetic resonance; [Trp^2]oxytocin, [tryptophan^2]oxytocin; [Tyr^2]oxytocin, [tyrosine^2]-oxytocin; NATrpA, *N*-acetyltryptophanamide; *t*-Boc, *tert*-butyloxycarbonyl; HPLC, high-pressure liquid chromatography; TFA, trifluoroacetic acid; TPPI, time-proportional phase increment; NOE, nuclear Overhauser effect; ROESY, rotating frame Overhauser enhancement spectroscopy.

terized in aqueous solution by NMR (Glickson et al., 1972, 1975; Richard-Brewster et al., 1973; Bradbury et al., 1974; Hruby, 1974; Wyssbrod et al., 1977) and fluorescence (Ross et al., 1986a), and there is a crystal structure of the desamino analogue (Pitts et al., 1985; Wood et al., 1986; Husain et al., 1990). With this body of information, we can compare the chemical and structural effects of the same surrounding sequence on tyrosine and tryptophan, respectively. This paper shows that, like [Tyr^2]oxytocin, there is a direct correlation between the preexponential weighting factors (amplitudes) of the three observed fluorescence decay constants of [Trp^2]-oxytocin and the three ^{1}H NMR-determined χ^1 rotamer populations of the Trp^2 side chain.

Materials and Methods

Peptide Synthesis. [Trp^2]oxytocin (Figure 2) was synthesized by the stepwise Merrifield procedure (Merrifield, 1963; Barany & Merrifield, 1980) using benzhydrylamine resin (Star Biochemicals) as the solid support (0.4 mmol of amine/g of resin). The *tert*-butyloxycarbonyl group (*t*-Boc) was used for N^{α} protection, and the 4-methylbenzyl group was used to protect the side chain of cysteine. A manual coupling protocol was followed (Merrifield et al., 1982), using a 3-fold molar excess of the preformed 1-hydroxybenzotriazole esters of the protected amino acids (Star Biochemicals). The extent of coupling was monitored by the qualitative ninhydrin test (Kaiser et al., 1970), which was negative after each cycle. After incorporation of the tryptophan residue, the solvent was changed to TFA/methylene chloride/anisole (5:4:1) to remove the *t*-Boc groups. *t*-Boc-$^{15}N'$-tryptophan (a kind gift from Dr. P. G. Katsoyannis) was used in one synthesis to prepare an isotopomer labeled at the α-amino group of tryptophan. Dithiothreitol (40 mg/mL) was also present to prevent destruction of the indole ring. After the chain was assembled and the α-amino terminal *t*-Boc group was removed, the resin was neutralized and dried in vacuo. A portion (0.5 g) was treated for an hour at 4 °C in a solution of 9 mL of liquid HF and 1 mL of *p*-cresol to remove the fully-deprotected peptide chain from the resin. HF was removed under reduced pressure, and the residue was then washed several times with cold ethyl acetate, once with petroleum ether, and dried in vacuo. The peptide was extracted from the residue with four 6-mL portions of 1 M acetic acid, and the combined extracts were washed with ethyl acetate. The resulting aqueous layer was diluted with 135 mL of water and adjusted to pH 9.0 with 1 M NH_4OH. After stirring for a day at room temperature (~22 °C) in an open vessel, allowing oxidation of the sulfhydryl groups under mild conditions, the slightly turbid mixture was lyophilized, yielding 90 mg of crude product.

[Trp^2]Oxytocin was purified by HPLC. A 5-mg portion of the crude product was dissolved in 1 mL of 0.1% TFA and filtered through a 0.45-μm filter. The sample was applied to a Vydac semipreparative C-18 column (1 × 25 cm) and chromatographed with a 0.1% TFA/acetonitrile gradient (5–50% acetonitrile, 80 min, 1.5 mL/min). The main peak, which eluted with a retention time of 40 min, was collected and lyophilized. The homogeneity of the material was checked by analytical HPLC (Hasselbacher et al., 1991b). By these criteria (230-nm detection), the peptide was greater than 99% pure. Amino acid analysis, following hydrolysis of the peptide in 6 N HCl for 1.5 h at 150 °C, yielded a composition of Asx (1.1 mol), Glx (1.0 mol), Gly (1.0 mol), Cys–Cys (0.8 mol), Ile (1.0 mol), Leu (1.0 mol), and Pro (0.9 mol) relative to Leu. Tryptophan was destroyed by the hydrolysis. This composition agrees with that expected for [Trp^2]oxytocin (see Figure 2). Also, the ^{1}H NMR spectrum of this peptide is consistent with that obtained for [Tyr^2]oxytocin [see Wyssbrod et al. 1977)].

Absorption and Steady-State Fluorescence Spectroscopy. Absorption spectra were measured at room temperature (~22 °C) using a U3210 Hitachi double-beam spectrophotometer. Technical steady-state fluorescence spectra were measured at 20 °C using an SLM/Aminco SPF 500C fluorometer equipped with a thermostated cuvette holder (±0.1 °C). The fluorometer was modified in our laboratory to use Glan–Thompson polarizers. Excitation and emission bandwidths were 4 and 5 nm, respectively.

Time-Resolved Fluorescence Spectroscopy. Fluorescence lifetimes were obtained at 20 °C by the time-correlated single-photon-counting method (Badea & Brand, 1981). Our instrument uses a frequency-doubled Rhodamine R6G dye laser (Spectra-Physics 375B) synch-pumped by a frequency-doubled, mode-locked Nd:YAG laser (Spectra-Physics 3460) as the excitation source [see Hasselbacher et al. (1991a)]. Decay curves were collected into 2000 channels at a resolution of 22 ps/channel. Both the steady-state and time-resolved fluorescence data were obtained under magic angle conditions to avoid intensity artifacts due to molecular rotation during the lifetime of the excited state (Paoletti & LePecq, 1969; Azumi & McGlynn, 1962; Kalantar, 1968; Shinitzky, 1972). Peptide concentrations were about 10^{-4} M ($A_{295} \approx 0.2$). All solutions were 0.001 M HCl. In this way, since the pK_a of the α-amino group of oxytocin is 6.3 (Hruby et al., 1977), we were exciting only one ionic form of the peptide.

Fluorescence Data Analyses. Fluorescence intensity decay curves were analyzed by nonlinear least-squares regression (Bevington, 1969), fitting the data to a sum of exponentials as expressed by

$$I(t) = \sum_{i=1}^{n} \alpha_i e^{-t/\tau_i} \qquad (1)$$

where α_i is the amplitude and τ_i is the lifetime of the ith component (Knight & Selinger, 1971, Grinvald & Steinberg, 1974). The reduced chi-squared value and weighted residuals with their autocorrelation were used as best fit criteria. The range of chi-squared values, which resulted in random weighted residuals and a random autocorrelation for the residuals, was 1.0–1.2 (unrestricted triple-exponential fits; see Results). The individual curves were also analyzed assuming a functional linkage among the weighting factors (amplitudes) of the individual decay constants (Ross et al., 1986b). The linkage was based on the ^{1}H NMR-determined ground-state rotamer populations (see below). Typically, one amplitude was iterated as an independent variable, while the linked amplitude(s) was scaled to the iterated amplitude. Sets of intensity decay curves obtained as a function of emission wavelength were also analyzed by a global nonlinear least-squares fitting procedure (Knutson et al., 1983; Beechem et al., 1983). In the global analysis, one or more of the decay constants was assumed to be emission wavelength independent and iterated as a common parameter for all curves. Finally, sets of curves were analyzed by the same global approach which included a functional linkage among the amplitudes (Ross et al., 1986b).

The fluorescence quantum yield from the integrated steady-state emission spectrum was compared with the number (amplitude) average lifetime, $\bar{\tau}$ (Förster, 1951; De Lauder & Wahl, 1970), expressed by

$$\bar{\tau} = \frac{\sum_{i=1}^{n} \alpha_i \tau_i}{\sum_{i=1}^{n} \alpha_i} \qquad (2)$$

Table I: Fluorescence Decay Parameters for [Tryptophan^2]Oxytocin[a]

data analysis model	α_1	τ_1 (ns)	α_2	τ_2 (ns)	α_3	τ_3 (ns)	$\langle\tau\rangle$ (ns)	$\bar{\tau}$ (ns)
individual curves[b]	0.39 ± 0.03	0.32 ± 0.02	0.42 ± 0.02	1.07 ± 0.05	0.19 ± 0.02	2.62 ± 0.09	1.70	1.07
common lifetimes[b,c]	0.39 ± 0.02	0.32	0.43 ± 0.01	1.08	0.18 ± 0.01	2.64	1.69	1.06
individual curves: linked amplitudes[b,d]	0.41	0.34 ± 0.03	0.41	1.12 ± 0.05	0.18	2.65 ± 0.06	1.70	1.08
common lifetimes: linked amplitudes[c,d]	0.41	0.35	0.41	1.13	0.18	2.66	1.70	1.09

[a] Samples were in 0.001 M HCl at 20 °C. The decay data were obtained as a function of emission wavelength (every 5 nm from 330 to 410 nm with a detection band-pass of 5 nm) with 295-nm excitation and a timing resolution of 22 ps/channel. In all analyses, the amplitudes are normalized to unity. [b] Standard deviations were calculated assuming that the iterated variables are independent of emission wavelength. [c] Three common, emission wavelength-independent lifetimes assumed. [d] Amplitude linkage based upon the ^{1}H NMR-determined χ^1 rotamer populations.

which is directly proportional to the ratio of the sum of the photons in the decay curve and the total number of excitation events; the relative intensity of each component i is $\alpha_i\tau_i/\bar{\tau}$. The mean lifetime, $\langle\tau\rangle$, which is an intensity-weighted average (Inokuti & Hirayama, 1965), is used, for example, in analysis of anisotropy decay (Dale et al., 1977) or time-resolved fluorescence quenching (Contino & Laws, 1991) and is defined by

$$\langle\tau\rangle = \frac{\sum_{i=1}^{n}\alpha_i\tau_i^2}{\sum_{i=1}^{n}\alpha_i\tau_i} \quad (3)$$

^{1}H NMR Spectroscopy and Calculation of Rotamer Populations. Samples, preexchanged in D_2O, were prepared by dissolving 1 mg of the peptide in 1 mL of D_2O and adjusting pD to 2.8 with DCl. ^{1}H NMR spectra were obtained on a Bruker AMX500 located at the Chemistry Department of the University of Louisville. All spectra were obtained at ambient temperature (~22 °C), and there was no evidence of high-order peptide aggregation. In most cases, presaturation was used to reduce the resonance due to residual H_2O. Chemical shift assignments were made by comparison with previous work on oxytocin (Wyssbrod et al., 1979) and by a two-dimensional phase-sensitive correlation spectroscopy experiment using the time-proportional phase incrementation method (TPPI) (Marion & Wüthrich, 1983). Coupling constants were obtained from standard one-dimensional ^{1}H spectra as well as from a selective one-dimensional version (Crouch & Martin, 1991) of the inverse heteronuclear long-range correlation experiment (Bax & Summers, 1986). In the latter, a selective ^{15}N pulse was applied at the resonance frequency of the ^{15}N′-label on Trp^2, omitting the low-pass filter (Crouch & Martin, 1991) since the solvent was D_2O and there is no one-bond N–H coupling. This experiment was used to help confirm the chemical shift assignments for tryptophan. The precision of the coupling constants obtained by these methods was ±0.2 Hz.

The fractional χ^1 populations p_I, p_{II}, and p_{III} (Figure 1) were calculated from the coupling constants between H^α and $H^{\beta R}$ ($H^{\beta S}$) (Pople, 1958; Pachler, 1963) according to (Wyssbrod et al., 1977; Fischman et al., 1978)

$$p_I = [^3J(H^\alpha\text{–}H^{\beta R}) - {}^3J_g]/\Delta^3J \quad (4)$$

$$p_{II} = [^3J(H^\alpha\text{–}H^{\beta S}) - {}^3J_g]/\Delta^3J \quad (5)$$

$$p_{III} = 1 - p_I - p_{II} = \{{}^3J_t + {}^3J_g - [^3J(H^\alpha\text{–}H^{\beta R}) + {}^3J(H^\alpha\text{–}H^{\beta S})]\}/\Delta^3J \quad (6)$$

where $\Delta^3J = {}^3J_t - {}^3J_g$, and ^3J_t and ^3J_g are the nominal values of the coupling constants for vicinal protons in trans and gauche conformations, respectively [see also Pachler (1964)].

The χ^1 populations were also calculated from the coupling between ^{15}N′ and $H^{\beta R}$ ($H^{\beta S}$) (Lichter & Roberts, 1970; Sogn et al., 1973) according to (Fischman et al., 1978)

$$p_I = [^3J(^{15}N'\text{–}H^{\beta S}) - {}^3J_g(^{15}N\text{–}^1H)]/\Delta^3J(^{15}N\text{–}^1H) \quad (7)$$

$$p_{III} = [^3J(^{15}N'\text{–}H^{\beta R}) - {}^3J_g(^{15}N\text{–}^1H)]/\Delta^3J(^{15}N\text{–}^1H) \quad (8)$$

$$p_{II} = 1 - p_I - p_{III} = \{{}^3J_t(^{15}N\text{–}^1H) + {}^3J_g(^{15}N\text{–}^1H) - [^3J(^{15}N'\text{–}H^{\beta S}) + {}^3J(^{15}N'\text{–}H^{\beta R})]\}/\Delta^3J(^{15}N\text{–}^1H) \quad (9)$$

where $\Delta^3J = {}^3J_t - {}^3J_g$, and ^3J_t and ^3J_g are the nominal values of the *heteronuclear* coupling constants for vicinal ^{15}N and ^{1}H nuclei in trans and gauche conformations, respectively [see also Lichter and Roberts (1970)].

Finally, to assess χ^2 conformations, a two-dimensional rotating frame nuclear Overhauser experiment (ROESY) (Bax & Davis, 1985) was carried out using presaturation and phase-sensitive detection processing with TPPI. ROESY is preferred over the basic NOE experiment because the rotational correlation time of [Trp^2]oxytocin is unfavorable for NOE. Mixing times of 150 and 300 ms gave similar results.

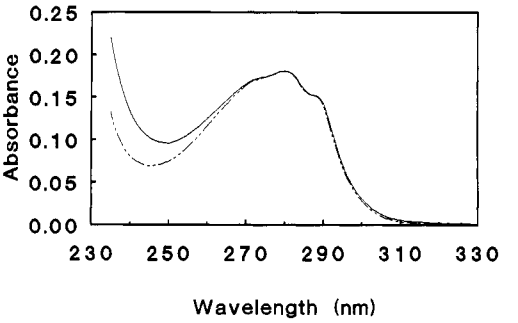

FIGURE 3: Absorption spectra of *N*-acetyltryptophanamide (- - -) and [Trp^2]oxytocin (—) at pH 3. Spectra have been normalized at 280 nm to facilitate comparison.

Results

Absorption and Steady-State Fluorescence. The pH 3 absorption spectra of [Trp^2]oxytocin and the model compound *N*-acetyltryptophanamide (NATrpA)[3] resemble each other closely in the wavelength region from 260 to 300 nm (Figure 3). The contribution of the disulfide bond between Cys^1 and Cys^6 to the absorption spectrum is much less prominent than in the native peptide [see Ross et al. (1986a)] because tryptophan absorption is much stronger than that of tyrosine and extends to lower energies. As shown in Figure 4, the fluorescence emission spectrum of [Trp^2]oxytocin has the same shape as that of NATrpA, but its maximum is shifted slightly to higher energy. Within the resolution of the excitation and

[3] Tryptophan residues in polypeptide chains generally have blocked α-amino and α-carboxyl groups due to the peptide linkage with adjacent amino acid residues. For this reason, NATrpA is commonly used as a model in studies on intrinsic protein fluorescence.

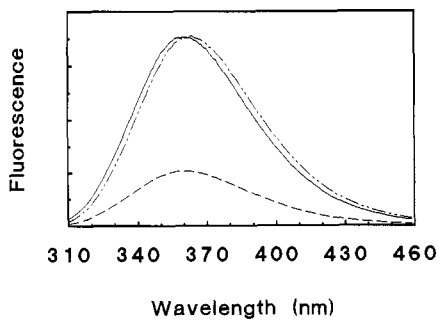

FIGURE 4: Uncorrected, area-normalized fluorescence emission spectra of *N*-acetyltryptophanamide (- - -) and [Trp^2]oxytocin (—) at pH 3. The lower spectrum (– –) shows the emission of [Trp^2]oxytocin scaled according to its quantum yield relative to that of *N*-acetyltryptophanamide.

detection band-passes (4 and 5 nm, respectively), the shapes of the emission spectra of both compounds are independent of excitation wavelength.

Time-Resolved Fluorescence. The fluorescence intensity decay of [Trp^2]oxytocin is complex, requiring three exponentials with time constants of about 0.3, 1.1, and 2.6 ns to fit the data adequately (Table I). The residuals for two-exponential fits were nonrandom, and the chi-squared values were 3-fold greater than those obtained for triple-exponential fits. When decay curves obtained every 5 nm between 330 and 410 nm are analyzed individually without imposing any assumptions other than that the intensity decay is a sum of exponentials, both the decay constants and the amplitudes of the 0.3- and 1.1-ns components appear to be independent of emission wavelength. In addition, the amplitude of the longest lived component is invariant with emission wavelength. The time constant of this component, however, appears to increase slightly toward the lower energy side of the spectrum. The trend is small, increasing from about 2.6 ns at 330 nm to 2.8 ns above 400 nm. The average values of the intensity decay parameters are given in Table I for unrestricted, single curve analyses of data obtained across the emission spectrum. The average values and standard deviations assume that all the parameters are wavelength independent. It should be noted that above 400 nm the values of longest lived component are within two standard deviations of its average value. Analyses for the sum of four exponentials (eight independent variables) yielded no improvement in statistical parameters, indicating that a triple-exponential decay law is sufficient.

To test in a more stringent way whether the three lifetimes vary as a function of emission wavelength, the decay curves were analyzed globally for three constant, common lifetimes. As shown in Table I, the values recovered from this global analysis for the common decay constants are indistinguishable from the average values of the decay constants recovered from the analyses of the individual decay curves. Inclusion of a fourth exponential slightly improved the fitting statistics of some curves in the data set. The improvement, however, was random with respect to emission wavelength, and the recovered parameters showed that the fourth exponential component was simply fitting noise.

Fluorescence Quantum Yield. The quantum yield of [Trp^2]oxytocin, calculated by integrating steady-state spectra, was found to be 32 ± 2% relative to NATrpA. From the number average lifetime of [Trp^2]oxytocin (eq 2) and the single-exponential lifetime of NATrpA, which under these experimental conditions is 3.0 ns, we calculated a relative quantum yield of 35 ± 2% for [Trp^2]oxytocin. Thus, within experimental error, the steady-state and number average lifetime quantum yields are the same.

^1H NMR. Figure 1 indicates the three main χ^1 conformations for the indole ring rotation about the C^α–C^β bond. To determine the ground-state populations of the rotamers, ^{1}H NMR studies were performed. Proton spectra were referenced relative to the HDO peak at 4.60 ppm. The following ^{1}H chemical shifts were found for the tryptophan residue in [Trp^2]oxytocin: H^α, 4.75 ppm; $H^{\beta D}$ (downfield H^β), 3.21 ppm; $H^{\beta U}$ (upfield H^β), 3.10 ppm; H^2, 7.14 ppm; and H^4, 7.54 ppm. The coupling constant (^3J) between $H^{\beta U}$ and H^α of the tryptophan residue in [Trp^2]oxytocin is 7.1 Hz, which is identical with the coupling constant between $H^{\beta D}$ and H^α. Clearly, stereochemical assignments of $H^{\beta R}$ and $H^{\beta S}$ are irrelevant because the couplings to H^α are the same. Consequently, it follows that the calculated populations for p_I and p_{II} will be the same. On the basis of the Pachler values for gauche and trans ^3J homonuclear couplings of 2.6 and 13.56 Hz, respectively (Pachler, 1964), $p_I = p_{II} = 0.41 \pm 0.03$, and $p_{III} = 0.18 \pm 0.05$.

Although stereochemical assignments of the H^βs are not necessary for determining χ^1 in this particular case, they are required for determining the χ^2 rotamers about the C^β–C^γ bond. We used heteronuclear couplings between the $^{15}N'$ and the H^βs to make these assignments *indirectly*. The coupling constant between $H^{\beta D}$ and $^{15}N'$ of the tryptophan residue in [$^{15}N'$-Trp^2]oxytocin is 2.6 Hz and that between $H^{\beta U}$ and $^{15}N'$ is 1.7 Hz. The first of two stereochemical assignments is for $H^{\beta S} = H^{\beta D}$ and for $H^{\beta R} = H^{\beta U}$. On the basis of the Sogn et al. (1973) values for gauche and trans ^3J heteronuclear couplings of 1.8 and 4.8 Hz, respectively, $p_I = 0.27 \pm 0.10$, $p_{III} = -0.03 \pm 0.10$, and $p_{II} = 1 - p_I - p_{III} = 0.76 \pm 0.15$. The second set of assignments reverses the first: $H^{\beta S} = H^{\beta U}$ and $H^{\beta R} = H^{\beta D}$. With this assignment, the values of p_I and p_{III} are interchanged. We have adopted the first set of assignments (see Discussion). It should be noted that nuclear Overhauser interactions between the H^α and H^βs consistent with the rotamer assignments were observed in ROESY spectra (see below).

Figure 1 also indicates the two main χ^2 conformations for the indole ring for rotation about the C^β–C^γ bond. For χ^2 of −90°, nuclear Overhauser interactions are expected between H^2 and $H^{\beta S(D)}$ and between H^4 and $H^{\beta R(U)}$; for χ^2 of +90°, nuclear Overhauser interactions are expected between H^2 and $H^{\beta R(U)}$ and between H^4 and $H^{\beta S(D)}$ (Dezube et al., 1981). The experimental ROESY spectra showed all of these interactions with roughly equal magnitude. Somewhat larger interactions were also observed between H^α and both H^2 and H^4. These observations are consistent with two χ^2 populations. Depending upon the degree of correlation between χ^2 and χ^1, there may be from three to six side-chain conformations for the tryptophan residue. As previously concluded by Dezube et al. (1981), the NOE data are qualitative in nature. While NOEs are excellent as observables for detecting specific interactions, they are not as precise as coupling constants for estimating populations.

Discussion

Fluorescence Decay Model for a Tryptophan Residue. The origins of the complex fluorescence decay behavior of single tryptophan residues in polypeptides and proteins have been the subject of considerable debate. Complex fluorescence intensity decay can result from either ground-state or excited-state heterogeneity, and understanding the processes that result in ground-state and/or excited-state heterogeneity is essential for accurate interpretation of tryptophan fluorescence decay kinetics. This understanding will also facilitate more

detailed investigations of protein structure and dynamics in solution.

In general, the fluorescence decays of simple aromatic hydrocarbons are single exponential when no heteroatoms are present in the ring of the molecule and strong interactions with the bulk solvent do not occur; an example is terphenyl in cyclohexane (Ross et al., 1981a). For those fluorophores that have excited-state solvation on the same time scale as the fluorescence decay, these interactions lead to nonexponential decay laws. When the fluorescence decay is analyzed by sums of exponentials and the resulting parameters are compared as a function of emission wavelength, there is no recognizable kinetic pattern to the individual time constants and their associated amplitudes. In addition, the average (or mean) lifetime increases with decreasing emission energy (DeToma et al., 1976; Lakowicz et al., 1980). This behavior has been ascribed to reorientation of the solvent molecules around the excited molecule to accommodate the different in the dipole moments of the ground state and the excited state of the solute (Bakhshiev, 1964). Molecular dynamics simulations of nonequilibrium solvation and time-resolved fluorescence of the first excited singlet state of formaldehyde suggest that in water the major relaxation occurs on a subpicosecond time scale (Levy et al., 1990). Indole, which contains nitrogen as a heteroatom and can readily interact with the solvent, exhibits single-exponential fluorescence decay in solvents such as cyclohexane or ethanol (De Lauder & Wahl, 1971) or water (Privat et al., 1985). Consequently, since indole in water exhibits a single fluorescence lifetime near 4.5 ns at 20 °C (Ross et al., 1981a; Privat et al., 1985), the emission of indole in water is from a fully solvent-relaxed excited state. Indole also undergoes other excited-state reactions, including proton transfer, electron transfer, and photoionization [see the review by Creed (1984)]. Since its fluorescence decay is single exponential, these processes are irreversible during the lifetime of the excited state and only contribute to nonradiative decay.

A considerable body of evidence has accumulated indicating that structural heterogeneity can result in complex fluorescence decay kinetics for tryptophan. For example, Donzel et al. (1974) studied the diketopiperazines *cyclo*-(–Gly–Trp–) and *cyclo*-(–Ala–Trp–) in dimethyl sulfoxide. They observed that each compound had two fluorescence lifetimes. The decay constants were independent of emission wavelength, while the amplitudes varied with emission wavelength. The amplitude variation suggested that the decay constants were associated with indolyl side chains in two chemically distinct environments. On this basis, each steady-state emission spectrum was resolved into two decay-associated spectra which were assigned to two possible side-chain conformers, one folded and the other extended. It has also been observed that the fluorescence intensity decays of a number of tryptophan model compounds are complex and can be fit by multiple exponentials (Szabo & Rayner, 1980; Ross et al., 1981a; Chang et al., 1983; Petrich et al., 1983). These exponentials have been attributed to χ^1 rotamers about the C^{α}–C^{β} bond that have different lifetimes as a result of specific interactions with the primary amide and carbonyl functions. In addition, Trp–X and X–Trp dipeptides show multiexponential fluorescence intensity decays. From consideration of factors such as the ionization state of the amino-terminal group and position of the Trp residue in the dipeptide, the rotamer model has been used to explain the differences observed in the lifetimes and amplitudes of the individual decay components (Chen et al., 1991).

While ground-state χ^1 rotamers have been suggested as the origin of the complex fluorescence decay of tryptophan zwitterion and model compounds, a direct correlation between the amplitudes and rotamer populations has not been demonstrated. In the case of tryptophan, there is the possibility of two χ^2 populations for each of the three χ^1 rotamers. Depending on the number of conformers (rotamers) that are populated, the rate of fluorescence decay of each population, and the rates for interconversion between conformers compared with the rates for the fluorescence decay of each population, as many as six different fluorescence decay times might be expected. It is difficult to predict how the fluorescence decay parameters will correlate with ground-state conformer populations. If interconversion between conformers occurs at rates similar or faster than fluorescence decay, if there are differences in the extinction coefficients of conformers at the excitation wavelength, or if the conformers have different emission spectra, then the observed fluorescence decay amplitudes will not be the same as the populations of the ground-state conformations. Furthermore, the ability of an analysis algorithm to extract all of the kinetic parameters correctly from the data must be questioned. For example, two or more conformers may have similar, unresolvable lifetimes. Depending upon the physical aspects of the situation as mentioned above, the quality of the data, and the robustness of the analysis, the decay data may be adequately fit to all statistical criteria by fewer components than the existing number of conformers. In these cases, resolving the appropriate kinetic mechanism will be difficult unless additional information is available to help guide the data analysis (Ross et al., 1988).

Ground-State Conformations of [Trp²]Oxytocin and the Fluorescence Decay Model. ^{1}H NMR spectroscopy, which was carried out *independently* of the initial fluorescence analyses, was used to assess the ground-state conformations of the tryptophan residue in [Trp²]oxytocin. The populations of rotamers I and II were found to be essentially equal and about twice that of rotamer III. This determination of the χ^1 rotamer populations stems from several considerations. The assignments of the resonances for the indole ring protons H^2 and H^4 are based on comparison with published assignments (Skrabal et al., 1979). Stereochemical assignments of the H^{β}s are based on *heteronuclear* couplings between these protons and $^{15}N'$. The assignment of $H^{\beta S}$ to $H^{\beta D}$ and $H^{\beta R}$ to $H^{\beta U}$ is more reasonable than the reverse assignment because it leads to $p_I > p_{III}$, which is in agreement with the populations calculated from *homonuclear* couplings. Moreover, our assignment is in agreement with stereochemical assignments made by Skrabal et al. (1979) for a series of simple tryptophan model compounds. (The only exception that they found was in a dipeptide where ring-current shifts caused a reversal in an assignment.) The assignments by Skrabal et al. (1979) are unequivocal because they studied a stereospecific isomer of L-tryptophan that had been synthesized with deuterium at $H^{\beta S}$ but not at $H^{\beta R}$.

We have also examined the χ^1 rotamer populations by using the nominal values for the heteronuclear coupling constants ^3J_t and ^3J_g. The value of p_{III} calculated from *heteronuclear* values is close to zero, while that from *homonuclear* values is around 0.18. Although it could be argued that these values may be within experimental error, especially when taking into consideration the low precision of the *heteronuclear* values, their difference may be real and significant and would thus indicate that the nominal literature values for heteronuclear ^3J_t and ^3J_g may not pertain to tryptophan. If we assume that the populations are correctly calculated from *homonuclear* couplings, then values for *heteronuclear* trans and gauche

couplings can be calculated from the equations used by Lichter and Roberts (1970). In this way, we find that $^3J_t(^{15}N-^1H)$ = 4.9 Hz, which is in close agreement with the literature values, and that $^3J_g(^{15}N-^1H)$ = 1.0 Hz, which is lower than the nominal literature values but within experimental error of the value proposed by Lichter and Roberts (1970).

One must consider that the NMR results could reflect a fixed conformation. To address this possibility, the four circumjacent homonuclear and heteronuclear coupling constants were analyzed by the intersection-of-sets method (Wyssbrod et al., 1977; Fischman et al., 1980) and the conformation-locus method (Wyssbrod, 1980). Karplus relationships between χ^1 and couplings that had been previously utilized by us to examine the cystine residue in oxytocin (Fischman et al., 1980) were used for these analyses. The results of the intersection-of-sets analysis were incompatible with a fixed conformation since the coupling constants did not yield a common, fixed conformational angle. The conformation-locus analysis was also incompatible with a fixed conformation since the coupling constants did not fall near the locus of a fixed conformation. We conclude, therefore, that the NMR results reflect averaged conformations.

The lower limit for the rate of χ^1 interconversion can be estimated from consideration of the chemical shifts of the tryptophan H^βs. Since an averaged spectrum is observed for both H^βs, rather than three individual spectra corresponding to each of the rotameric forms, the rotamers are interconverting rapidly on the NMR time scale. This time scale is determined by the range of chemical shift expected for each H^β. From an examination of chemical shifts observed in a variety of tryptophan-containing compounds, we expect the range of chemical shift to be on the order of 0.5 ppm, which corresponds to 1570 rad s^{-1} at 500 MHz. Thus, we expect the lower limit for the rate of interconversion to be within an order of magnitude of 10^3 s^{-1}.

Upon comparing these NMR results with the independent parameters obtained from the initial analyses of the individual fluorescence intensity decay curves, we were intrigued by the agreement between the χ^1 rotamer populations and the average values for the amplitudes of the three fluorescence intensity decay constants. This correlation between populations and amplitudes can be interpreted in several ways: (1) each χ^1 rotamer has only one χ^2 rotamer population; (2) the local interactions with the tryptophan side chain are imposed by χ^1 and there is no influence of the χ^2 orientation on the fluorescence lifetime; or (3) the rates of interconversion between χ^2 rotamers are fast compared to the rates of fluorescence decay, thus averaging out the influence of χ^2 orientation upon the nonradiative decay rates. Of course, it is also possible that the unrestricted fluorescence decay analysis results are not unique, the parameters merely fit the data, and the amplitudes coincidentally match the NMR-determined rotamer populations.

Several approaches were taken to analyze the fluorescence decay curves to examine the apparent correlation between the recovered parameters and χ^1 rotamer populations (Table I). First, the decay curves collected as a function of emission wavelength were analyzed individually with the amplitudes linked to the NMR-determined rotamer populations (Ross et al., 1986b). In this approach there are four independent parameters (three lifetimes and one amplitude), and the other two amplitudes are calculated relative to the iterated amplitude. In general, the fitting statistics obtained using this linkage were indistinguishable from those obtained fitting the data for six unrestricted parameters (three lifetimes and their associated amplitudes). The second test of this model included no assumptions about the relative values for the amplitudes of the decay constants obtained for the individual decay curves. Instead, the fluorescence decay constants were assumed to be independent of emission wavelength and common to all decay curves. The overall fitting statistics for this global analysis (Knutson et al., 1983; Beechem et al., 1983) were worse for decay curves obtained on the low- and high-energy sides of the emission spectrum, suggesting a trend in one or more of the lifetimes or a systematic error in the data. When the same analysis was carried out assuming only two common, emission wavelength–independent lifetimes, there was improvement in the global fit, and the longest lifetime, which is associated with the smallest amplitude, showed a tendency to increase with increasing emission wavelength (200-ps increase between 330 and 410 nm). This increase had also been noted in the single curve analyses with six independent parameters. It is not clear at the present time whether this increase reflects a small systematic error, other kinetic processes such as relaxation, some additional conformational heterogeneity, slightly different emission spectra for the rotamers, or inability of the analysis algorithm to distinguish six time constants (for six different environments) when there are three pairs of similar values. What is clear is that the relative amplitudes obtained in both of these global analyses for common lifetimes are indistinguishable from those obtained from the unrestricted single curve analyses. This was confirmed by a global analysis in which the amplitudes were linked to the NMR-determined χ^1 populations and two of the lifetimes were held common.

The strong correlation between the amplitude terms and the ground-state χ^1 rotamer populations, regardless of the stringency imposed on the data analysis, and the absence of a need for a consistent set of additional decay components together suggest that the χ^1 rotamer model is sufficient to explain the [Trp^2]oxytocin fluorescence intensity decay data. This implies, first, that rotations about the tryptophan C^α–C^β bond have an upper limit of about 5×10^7 s^{-1} since the ground-state χ^1 populations have not changed following excitation to the first excited singlet state. This limit can be estimated from rate constants of systems known to undergo excited-state reactions and that have similar excited-state lifetimes. An example is the excited-state proton transfer of 2-naphthol (Laws & Brand, 1979). This should be contrasted with the lower limit for the rate of χ^1 rotation of about 10^3 s^{-1}, discussed previously. Second, this implies that the absorption and emission spectra of the three χ^1 rotamers are very similar. Third, the χ^1 rotamer model implies that the combined fluorescence and NMR results are consistent with either the χ^2 rotations being fast compared to the fluorescence intensity decay of the tryptophan residue, fluorescence intensity decay properties being dominated by χ^1 interactions, or the χ^2 and χ^1 rotations being highly correlated such that each χ^1 rotamer has predominantly one χ^2 conformation. It should be recognized, however, that these conclusions pertain only to [Trp^2]oxytocin. It remains to be seen whether these conclusions also apply to tryptophan residues in other polypeptides and proteins.

Fluorescence Intensity Decays of [Trp^2]Oxytocin and [Tyr^2]Oxytocin. Our previous studies on the fluorescence decay of several tyrosine model compounds and [Tyr^2]oxytocin showed that, under conditions where only one ionic form exists in solution, the relative amplitudes of the decay constants correlate quite well with the NMR-determined χ^1 populations of the phenol ring (Laws et al., 1986; Ross et al., 1986a). The results obtained from unrestricted analysis of the [Trp^2]-oxytocin fluorescence decay curves were initially compared

with the results which we had previously obtained for [Tyr^2]oxytocin (Ross et al., 1986a). We find two important differences. First, while the tyrosine fluorescence intensity decay can be fit by a double exponential, the tryptophan fluorescence data requires a triple exponential for an adequate fit. Second, comparison of steady-state fluorescence relative quantum yields with the number average lifetimes shows that whereas the tyrosine residue is involved in a static quenching interaction,[4] the tryptophan residue does not exhibit any evidence for static quenching.

From the X-ray crystal structure model of desaminooxytocin (Pitts et al., 1985), it appears that the phenol ring of tyrosine in both χ^1 rotamers I and II can come in close proximity to the disulfide bridge of the peptide hormone. Since disulfides are known quenchers of tyrosine and tryptophan fluorescence [see reviews by Longworth (1971), Cowgill (1976), and Ross et al. (1991)], and on the basis of the amplitude ratios for the two decay components of [Tyr^2]oxytocin and the correlation between fluorescence decay constants and rotamers of tyrosine model compounds (Laws et al., 1986), we argued that rotamer I was statically quenched in [Tyr^2]oxytocin (Ross et al., 1986a). The two observed lifetimes were associated with rotamer II (0.7-ns component) and rotamer III (1.9-ns component). This assignment was supported by the observations that desaminodicarbaoxytocin, in which the disulfide is replaced by the nearly isosteric ethylene bridge, shows no static quenching of its tyrosine and its fluorescence intensity decay can be fit by a sum of three exponentials with amplitudes that agree with the NMR-determined χ^1 rotamer populations.[5]

The presence of static quenching in [Tyr^2]oxytocin as opposed to [Trp^2]oxytocin can be explained in terms of a model based on the quenching of rotamer I by a highly efficient, dynamic process, such as resonance energy transfer to the disulfide chromophore. Molecular graphics modeling, based on the X-ray crystal structure of desaminooxytocin (Pitts et al., 1985), suggests that like tyrosine the aromatic ring of tryptophan at position 2 can be close to the disulfide bridge in certain rotamer conformations. If rotamer interconversion is slow compared to the time scale of fluorescence, highly efficient dynamic quenching of one rotamer would be indistinguishable from static quenching. Because of the overlap between the disulfide absorption band and the emission bands of both tyrosine and tryptophan, it is possible for quenching to occur via resonance energy transfer. Fluorescence of tyrosine, however, has greater spectral overlap with the disulfide absorption band, especially compared to the fluorescence of a fully solvent-exposed tryptophan. Assuming that the dipole–dipole orientation factor and distance of separation between donor and acceptor are similar, tyrosine will be more efficiently quenched than tryptophan. Also, in a rotamer where the aromatic side chain can come in close proximity to the disulfide bridge, energy transfer may proceed by the exchange interaction. The probability for exchange depends upon the overlap and details of the donor and acceptor wave functions (Inokuti & Hirayama, 1965; Dexter, 1953). Regardless of which resonance energy transfer mechanism dominates, it is expected that the quenching efficiency of tyrosine and tryptophan will differ. Less efficient energy transfer, which means a slower rate of deactivation of the excited state of the donor (tryptophan), could result in the appearance (resolution) of a third, relatively short lifetime. This would be consistent with the lack of static quenching of [Trp^2]oxytocin and a very short lifetime for rotamer I. Chen et al. (1991) have used a similar argument to explain the lifetime and amplitude differences observed for several Trp–X and X–Trp dipeptides.

In conclusion, the fluorescence intensity decay of [Trp^2]-oxytocin can be satisfactorily understood by the same rotamer model that we applied to [Tyr^2]oxytocin (Ross et al., 1986a). Our results for the tryptophan analogue suggest that its χ^2 conformers have little, if any, impact upon the fluorescence decay kinetics. They also suggest that, in the general case, when all three χ^1 rotamers of tryptophan are populated in the ground state, three decay constants may be observed.

[Trp^2]Oxytocin is only one polypeptide in which time-resolved fluorescence has been combined with NMR to investigate the basis for multiexponential fluorescence intensity decay of a single tryptophan residue. To test these conclusions further, it is important that other single tryptophan-containing polypeptides be studied by the same approach. There are additional ways to test this model. For example, rotamer populations should be temperature dependent. It should be noted, however, that the rotamer populations of [Tyr^2]oxytocin are essentially temperature independent between 0 and 60 °C (Wyssbrod et al., 1977). Another approach is dynamic fluorescence quenching, which has been used to study rotamer populations of tyrosinamide (Contino & Laws, 1991). According to the rotamer model, each lifetime is expected to decrease as a function of quencher concentration in accord with the Stern–Volmer relationship, but the amplitudes should be unaffected. Quenching experiments were currently underway in our laboratory comparing [Tyr^2]oxytocin with [Trp^2]-oxytocin.

In a more sterically-constrained system, only one or two χ^1 rotamers might be populated, suggesting that the fluorescence intensity decay of a single tryptophan residue might be mono- or biexponential. This would be consistent, for example, with the results indicating single-exponential fluorescence decays for the buried and exposed tryptophan residues of horse liver alcohol dehydrogenase, Trp^{314} and Trp^{15}, respectively (Ross et al., 1981b) or for the single buried tryptophan of apo forms of the homologous azurins from *Pseudomonas fluorescens* and *Pseudomonas aeruginosa* (Grinvald et al., 1975; Petrich et al., 1987; Hutnik & Szabo, 1989). In this regard, it is worth commenting that in our preliminary investigation of the fluorescence decay kinetics of two different insulin analogues in which tryptophan has been substituted for Tyr^{14} in the A chain, the tryptophan fluorescence intensity decay of both analogues is best fit by the same three decay constants (Ohta et al., 1990). The respective amplitudes of the identical time constants differ, however, which is consistent with a different mixture of χ^1 rotamers for the tryptophan in each analogue. Moreover, it is of interest that these two insulin analogues differ 4–5-fold in biological activity (P. G. Katsoyannis, personal communication). Thus, with our present results for

[4] Static quenching is operationally defined in terms of a nonradiative, ground-state complex with a characteristic equilibrium constant (Noyes, 1961). This can be conceptually extended to an equilibrium among rotamer populations in which one population is quenched by a very efficient nonradiative process.

[5] In our time-resolved fluorescence and ^{1}H NMR studies of the tyrosine residue in oxytocin (Ross et al., 1986a), we stated (under Results on page 609) that "the ^{1}H NMR spectrum of desaminooxytocin is ... complicated ... due to the extra hydrogen on the C$^\alpha$ of residue 1. Therefore, the phenol rotamer populations of desaminodicarbaoxytocin have not been determined...". Here, desaminodicarbaoxytocin is a misprint and was meant to be desaminooxytocin. We did resolve the phenol rotamer populations of desaminodicarbaoxytocin [Table II of Ross et al. (1986a)], even though its ^{1}H NMR spectrum was also complex due to the extra hydrogen on the C$^\alpha$ of residue 1. The ^{1}H NMR spectrum of desaminooxytocin, however, is even more complicated because its C$^\alpha$ hydrogens are shifted into the region of the aromatic resonances by interaction with the disulfide group. Thus, it was difficult to make accurate resonance assignments.

[Trp^2]oxytocin, there is an excellent prospect that the fluorescence intensity decay kinetics of tryptophan residues will prove valuable for investigations on protein structure and function.

ACKNOWLEDGMENTS

We thank Mark Lulka for help in preliminary studies, and we gratefully acknowledge Drs. Carol Hasselbacher and Evan Waxman for their critical reading of the manuscript. We also appreciate the helpful comments of one of the reviewers.

Registry No. [Trp^2]oxytocin, 37883-08-2; Trp, 73-22-3.

REFERENCES

Azumi, T., & McGlynn, S. P. (1962) *J. Chem. Phys. 37*, 2413–2420.

Badea, M. G., & Brand, L. (1979) *Methods Enzymol. 61*, 378–425.

Bakhshiev, N. G., Mazurenko, Y. T., & Piterskaya, I. V. (1966) *Opt. Spectrosk. 21*, 550–554.

Barany, G., & Merrifield, R. B. (1980) in *The Peptides: Analysis, Synthesis, Biology* (Gross, E., & Meinhofer, J., Eds.) pp 1–284, Academic Press, New York.

Bax, A., & Davis, D. G. (1985) *J. Magn. Reson. 63*, 207–213.

Bax, A., & Summers, M. F. (1986) *J. Am. Chem. Soc. 108*, 2093–2094.

Beechem, J. M., & Brand, L. (1985) *Annu. Rev. Biochem. 54*, 43–71.

Beechem, J. M., Knutson, J. R., Ross, J. B. A., Turner, B. W., & Brand, L. (1983) *Biochemistry 22*, 6054–6058.

Bevington, P. R. (1969) *Data Reduction and Error Analysis for the Physical Sciences*, McGraw-Hill, New York.

Bradbury, A. F., Burgen, A. S. V., Feeney, J., Roberts, G. C. K., & Smyth, D. G. (1974) *FEBS Lett. 42*, 179–182.

Brändén, C.-I., Jornvall, H., Eklund, H., & Furugren, B. (1975) *Enzymes (3rd Ed.) 11*, 103–190.

Chang, M. C., Petrich, J. E., McDonald, D. B., & Fleming, G. R. (1983) *J. Am. Chem. Soc. 105*, 3819–3824.

Chen, R. F., Knutson, J. R., Ziffer, H., & Porter, D. (1991) *Biochemistry 30*, 5184–5195.

Colucci, W. J., Tilstra, L., Sattler, M. C., Fronczek, F. R., & Barkley, M. D. (1990) *J. Am. Chem. Soc. 112*, 9182–9190.

Contino, P. B., & Laws, W. R. (1991) *J. Fluoresc. 1*, 5–13.

Cowgill, R. W. (1976) in *Biochemical Fluorescence: Concepts 2* (Chen, R. F., & Edelhoch, H., Eds.) pp 441–486, Marcel Dekker, New York.

Creed, D. (1984) *Photochem. Photobiol. 39*, 537–562.

Crouch, R. C., & Martin, G. E. (1991) *J. Magn. Reson. 92*, 189–194.

Dale, R. E., Chen, L. A., & Brand, L. (1977) *J. Biol. Chem. 252*, 7500–7510.

De Lauder, W. B., & Wahl, Ph. (1970) *Biochemistry 9*, 2751–2754.

De Lauder, W. B., & Wahl, Ph. (1971) *Biochim. Biophys. Acta 243*, 153–163.

DeToma, R. P., Easter, J. H., & Brand, L. (1976) *J. Am. Chem. Soc. 98*, 5001–5007.

Dexter, D. L. (1953) *J. Chem. Phys. 21*, 836–850.

Dezube, B., Dobson, C. M., & Teague, C. E. (1981) *J. Chem. Soc., Perkin Trans. 2*, 730–735.

Donzel, B., Gauduchon, P., & Wahl, Ph. (1974) *J. Am. Chem. Soc. 96*, 801–808.

Eftink, M. R., & Hagaman, K. A. (1986) *Biochemistry 25*, 6631–6637.

Fischman, A. J., Wyssbrod, H. R., Agosta, W. C., & Cowburn, D. (1978) *J. Am. Chem. Soc. 100*, 54–58.

Fischman, A. J., Live, D. H., Wyssbrod, H. R., Agosta, W. C., & Cowburn, D. (1980) *J. Am. Chem. Soc. 102*, 2533–2539.

Förster, T. (1951) *Fluoreszenz Organischer Verbindungen*, Vandenhoeck und Ruprecht, Göttingen, Germany.

Glickson, J. D. (1975) in *Peptides: Chemistry, Structure, and Biology* (Walter, R., & Meienhofer, J., Eds.) pp 787–802, Ann Arbor Science Publishers, Ann Arbor, MI.

Glickson, J. D., Urry, D. W., Havran, R. T., & Walter, R. (1972) *Proc. Natl. Acad. Sci. U.S.A. 69*, 2136–2140.

Grinvald, A., & Steinberg, I. Z. (1974) *Anal. Biochem. 59*, 583–598.

Grinvald, A., & Steinberg, I. Z. (1976) *Biochim. Biophys. Acta 427*, 663–678.

Grinvald, A., Schlessinger, J., Pecht, I., & Steinberg, I. Z. (1975) *Biochemistry 14*, 1921–1929.

Hasselbacher, C. A., Waxman, E., Galati, L. T., Contino, P. B., Ross, J. B. A., & Laws, W. R. (1991a) *J. Phys. Chem. 95*, 2995–3005.

Hasselbacher, C. A., Schwartz, G. P., Glass, J. D., & Laws, W. R. (1991b) *Int. J. Polypept. Protein Res. 38*, 459–468.

Hruby, V. J. (1974) in *Chemistry and Biochemistry of Amino Acids, Peptides, and Proteins* (Weinstein, B., Ed.) Vol. 3, pp 1–188, Marcel Dekker, New York.

Hruby, V. J., Yamamoto, D. M., Yang, Y. C. S., & Blumenstein, M. (1977) in *Peptides—Proceedings of the Fifth American Peptide Symposium* (Goodman, M., & Meienhofer, J., Eds.) pp 179–182, John Wiley & Sons, New York.

Husain, J., Blundell, T. L., Cooper, S., Pitts, J. E., Tickle, I. J., Wood, S. P., Hruby, V. J., Fischman, A. J., Wyssbrod, H. R., & Mascarenhas, Y. (1990) *Phil. Trans. R. Soc. London B 327*, 625–654.

Hutnik, C. M., & Szabo, A. G. (1989) *Biochemistry 28*, 3923–3934.

Inokuti, M., & Hirayama, F. (1965) *J. Chem. Phys. 43*, 1978–1989.

James, D. R., & Ware, W. R. (1985) *Chem. Phys. Lett. 120*, 450–454.

Kaiser, E., Colescott, R. L., Bossinger, C. D., & Cook, P. I. (1970) *Anal. Biochem. 34*, 595–598.

Kalantar, A. H. (1968) *J. Chem. Phys. 48*, 4992–4996.

Knight, A. E. W., & Selinger, B. K. (1971) *Spectrochim. Acta 27*, 1223–1234.

Knutson, J. R., Walbridge, D. G., & Brand, L. (1982) *Biochemistry 21*, 4671–4679.

Knutson, J. R., Beechem, J. M., & Brand, L. (1983) *Chem. Phys. Lett. 102*, 501–507.

Konev, S. V. (1967) *Fluorescence and Phosphorescence of Proteins and Nucleic Acids*, Plenum Press, New York.

Lakowicz, J. R., Cherek, H., & Bevan, D. R. (1980) *J. Biol. Chem. 255*, 4403–4406.

Lami, H., & Glasser, N. (1984) *J. Chem. Phys. 84*, 597–604.

Laws, W. R., & Brand, L. (1979) *J. Phys. Chem. 83*, 795–802.

Laws, W. R., Ross, J. B. A., Wyssbrod, H. R., Beechem, J. M., Brand, L., & Sutherland, J. C. (1986) *Biochemistry 25*, 599–607.

Leonard, L. J., & Forster, L. S. (1974) *Photochem. Photobiol. 19*, 353–360.

Levy, R. M., Kitchen, D. B., Blair, J. T., & Krogh-Jespersen, K. (1990) *J. Phys. Chem. 94*, 4470–4476.

Lichter, R. L., & Roberts, J. D. (1970) *J. Org. Chem. 35*, 2806–2807.

Longworth, J. W. (1971) in *Excited States of Proteins and Nucleic Acids* (Steiner, R. F., & Weinryb, I., Eds.) pp 319–484, Plenum Press, New York.

Marion, D., & Wüthrich, K. (1983) *Biochem. Biophys. Res. Commun. 113*, 967–974.
Merrifield, R. B. (1963) *J. Am. Chem. Soc. 85*, 2149–2154.
Merrifield, R. B., Vizioli, L. D., & Boman, H. G. (1982) *Biochemistry 21*, 5020–5031.
Noyes, R. M. (1961) *Prog. React. Kinet. 1*, 130–160.
Ohta, N., Zong, L., Katsoyannis, P. G., Laws, W. R., & Ross, J. B. A. (1990) *Biophys. J. 57*, 56a.
Pachler, K. G. R. (1963) *Spectrochim. Acta 19*, 2085–2092.
Pachler, K. G. R. (1964) *Spectrochim. Acta 20*, 581–587.
Paoletti, J., & LePecq, J.-B. (1969) *Anal. Biochem. 31*, 33–41.
Petrich, J. W., Chang, M. C., McDonald, D. B., & Fleming, G. R. (1983) *J. Am. Chem. Soc. 105*, 3824–3832.
Petrich, J. W., Longworth, J. W., & Fleming, G. R. (1987) *Biochemistry 26*, 2711–2722.
Philips, L. A., Webb, S. P., Martinez, S. J., III, Fleming, G. R., & Levy, D. H. (1988) *J. Am. Chem. Soc. 110*, 1352–1355.
Pitts, J. E., Wood, S., Tickle, I. J., Treharne, A.-M., Mascarenhas, Y., Li, J. Y., Husain, J., Cooper, S., Blundell, T., Hruby, V. J., & Wyssbrod, H. R. (1985) in *Peptides, Structure and Function, Proceedings* of *the Ninth American Peptide Symposium* (Deber, C. M., Hruby, V. J., & Kopple, K. D., Eds.) pp 145–150, Pierce Chemical Co., Rockford, IL.
Platt, J. F. (1949) *J. Chem. Phys. 17*, 484–495.
Platt, J. F. (1951) *J. Chem. Phys. 19*, 101–118.
Pople, J. A. (1958) *Mol. Phys. 1*, 3–8.
Privat, J. P., Wahl, Ph., & Brochon, J. C. (1985) *Biochimie 67*, 949–958.
Rayner, D. M., & Szabo, A. G. (1978) *Can. J. Chem. 56*, 743–745.
Rehms, A. A., & Callis, P. R. (1987) *Chem. Phys. Lett. 140*, 83–89.
Richard-Brewster, A. I., & Hruby, V. J. (1973) *Proc. Natl. Acad. Sci. U.S.A. 70*, 3806–3809.
Robbins, R. J., Fleming, G. R., Beddard, G. S., Robinson, G. W., Thistlethwaite, P. J., & Woolfe, G. J. (1980) *J. Am. Chem. Soc. 102*, 6271–6279.
Ross, J. B. A., Rousslang, K. W., & Brand, L. (1981a) *Biochemistry 20*, 4361–4369.
Ross, J. B. A., Schmidt, C. J., & Brand, L. (1981b) *Biochemistry 20*, 4369–4377.
Ross, J. B. A., Laws, W. R., Buku, A., Sutherland, J. C., & Wyssbrod, H. R. (1986a) *Biochemistry 25*, 607–612.
Ross, J. B. A., Laws, W. R., Sutherland, J. C., Buku, A., Katsoyannis, P. G., Schwartz, I. L., & Wyssbrod, H. R. (1986b) *Photochem. Photobiol. 44*, 365–370.
Ross, J. B. A., Laws, W. R., & Wyssbrod, H. R. (1988) *SPIE Vol. 909 Time-Resolved Laser Spectroscopy in Biochemistry*, 82–89.
Ross, J. B. A., Laws, W. R., Rousslang, K. W., & Wyssbrod, H. R. (1991) in *Topics in Fluorescence Spectroscopy, Vol. 3: Biochemical Applications* (Lakowicz, J. R., Ed.) pp 1–63, Plenum, New York.
Saito, I., Sugihama, H., Yamamoto, A., Muramatsu, S., & Matsuura, T. (1984) *J. Am. Chem. Soc. 106*, 4286–4287.
Shinitzky, M. (1972) *J. Chem. Phys. 56*, 5979–5981.
Shizuka, H., Serizawa, M., Shimo, T., Saito, I., & Matsuura, T. (1988) *J. Am. Chem. Soc. 110*, 1930–1934.
Sipior, J., Sulkes, M., Auerbach, R., & Boivineau, M. (1987) *J. Phys. Chem. 91*, 2016–2018.
Skrabal, P., Rizzo, V., Baici, A., Bangerter, F., & Luisi, P. L. (1979) *Biopolymers 18*, 995–1008.
Sogn, J. A., Gibbons, W. A., & Randall, E. W. (1973) *Biochemistry 12*, 2100–2105.
Strickland, E. H., Horwitz, J., & Billups, C. (1970) *Biochemistry 9*, 4914–4921.
Strickland, E. H., Billups, C., & Kay, E. (1972) *Biochemistry 11*, 3654–3662.
Sun, M., & Song, P.-S. (1977) *Photochem. Photobiol. 25*, 3–9.
Suzuki, S., Fujii, T., Imai, A., & Akahori, H. (1977) *J. Phys. Chem. 81*, 1592–1598.
Szabo, A. G., & Rayner, D. M. (1980) *J. Am. Chem. Soc. 102*, 554–563.
Tatischeff, I., Klein, R., Zemb, T., & Duquesne, M. (1978) *Chem. Phys. Lett. 54*, 394–397.
Tilstra, L., Sattler, M. C., Cherry, W. R., & Barkley, M. D. (1990) *J. Am. Chem. Soc. 112*, 9176–9182.
Valeur, B., & Weber, G. (1977) *Photochem. Photobiol. 25*, 441–444.
Wagner, B. D., James, D. R., & Ware, W. R. (1987) *Chem. Phys. Lett. 138*, 181–184.
Wood, S. P., Tickle, I. J., Treharne, A. M., Pitts, J. E., Mascarenhas, Y., Li, J. Y., Husain, J., Cooper, S., Blundell, T. L., Hruby, V. J., Buku, A., Fischman, A. J., & Wyssbrod, H. R. (1986) *Science 232*, 633–636.
Wyssbrod, H. R. (1980) in *Peptides: Synthesis–Structure–Function* (Rich, D. H., & Gross, E., Eds.) pp 261–265, Pierce Chemical Co., Rockford, IL.
Wyssbrod, H. R., Ballardin, A., Schwartz, I. L., Walter, R., Van Binst, G., Gibbons, W. A., Agosta, W. C., Fields, F. H., & Cowburn, D. (1977) *J. Am. Chem. Soc. 99*, 5273–5276.
Wyssbrod, H. R., Fischmann, A. J., Smith, C. W., & Walter, R. (1979) in *The Peptides: Structure and Biological Function* (Gross, E., & Meinhofer, J., Eds.) pp 213–216, Academic Press, New York.